Tuning the dye aerosol impaction and TiO$_2$ nanoparticle stacking structures for High-Efficiency Dye-Sensitized solar cells

Juan Zhang [a,1], Jung Keun Cha [a,1], Xiuting Luo [a], Eun Ji Cho [a], Ji Hoon Kim [b], Soo Hyung Kim [a,b,c,*]

[a] Department of Nanofusion Technology, Pusan National University, 2, Busandaehak-ro 63beon-gil, Geumjeong-gu, Busan 46241, Republic of Korea
[b] Research Center for Energy Convergence Technology, Pusan National University, 2, Busandaehak-ro 63beon-gil, Geumjeong-gu, Busan 46241, Republic of Korea
[c] Department of Nanoenergy Engineering, Pusan National University, 2, Busandaehak-ro 63beon-gil, Geumjeong-gu, Busan 46241, Republic of Korea

ARTICLE INFO

ABSTRACT

The rapid manufacturing of high-efficiency dye-sensitized solar cells (DSSCs) is limited by the slow dye adsorption on TiO$_2$ nanoparticles (NPs)-accumulated photoelectrode using conventional dip-coating process. Therefore, we aim to accelerate the adsorption of dyes that are attached on TiO$_2$ NPs by employing an aerosol impactor. Herein the aerosolized dyes are designed to get deposited rapidly on the TiO$_2$ NPs-accumulated photoelectrode. In addition, to effectively trap the irradiated sunlight in DSSCs, we assemble the photoelectrodes incorporated with bilayered TiO$_2$ thin films comprising small TiO$_2$ NPs-based underlayer and large TiO$_2$ NPs-based overlayer as dye-supporting and light-scattering mediums, respectively. Furthermore, the effects of dye aerosol impaction and TiO$_2$ stacking structures on the efficiency of DSSCs are examined. The power conversion efficiency (PCE) of DSSCs comprising a N719 dye-supporting layer treated with dip-coating process was determined as $\sim$ 5.67%; however, when the bilayered TiO$_2$ thin films with an optimized thickness ratio of light-scattering overlayer and dye-supporting underlayer were coated with N719 dyes using dye aerosol impactor, the resulting PCE increased to $\sim$ 7.46%. This suggests that the photovoltaic characteristics of DSSCs can be enhanced considerably using the effective TiO$_2$ NP stacking structures coated with rapid, uniform, and strong aerosol dye adsorption throughout the TiO$_2$-based photoelectrodes.

© 2021 The Society of Powder Technology Japan. Published by Elsevier BV and The Society of Powder Technology Japan. All rights reserved.

1. Introduction

Dye-sensitized solar cells (DSSCs) have attracted significant attraction as next generation photovoltaic cell owing to their simple structure, industrial mass production, and easy, non-toxic, and pollution-free manufacturing processes than those of the other conventional solar cells [1–4]. DSSCs consist of transparent conductive substrate, semiconductor oxide thin film, dye sensitizer, counter electrode, and redox electrolyte. Among these, semiconductor oxide thin film, which is in contact with the redox electrolyte, plays a vital role. Generally, TiO$_2$ nanoparticles (NPs)-accumulated thin film is used as a photoelectrode in DSSCs owing to its non-toxicity and chemical stability [5–8]. Dye sensitizers attached on TiO$_2$ NPs absorb irradiated light and generate electrons

and holes. The generated electrons are introduced into TiO$_2$, whereas the holes remain on the dye surface. Then, dye sensitizers are regenerated by electron supply from electrolyte, wherein the iodide is recovered by the reduction of triiodide on the counter electrode. Finally, a complete electric circuit is obtained when the electrons return from the external loads. Throughout this process, total state of the reactants remains unchanged, and light energy is converted into electrical energy [9–12].

Several researches have been conducted to optimize the size and structure of TiO$_2$, develop new dye sensitizers, and suppress charge recombination for enhancing the efficiency of DSSCs [13–15]. Among them, the effect of altering the TiO$_2$-based photoelectrodes on the performance of DSSCs has been investigated extensively. One of the strategies used for altering the TiO$_2$ photoelectrodes is to add a light-scattering overlayer, which consists of large primary TiO$_2$ NPs, on the top of a dye-supporting underlayer, which consists of small primary TiO$_2$ NPs [16–19]. The incident light can be effectively confined in the photoelectrodes by the presence of light-scattering overlayer, and thus, the dye molecules generate more electrons. Generally, TiO$_2$ NPs with large primary size increase the

light-scattering effect. However, increasing the thickness (or amount) of light-scattering layer with large primary TiO$_2$ NPs can decrease the specific surface area available for adsorbing the dyes. Simultaneously, the photogenerated electrons should pass through more conformal particles and grain boundaries, which can increase the possibility of charge recombination. Therefore, it is crucial to determine the optimized thickness of light-scattering overlayer in DSSCs. After precisely altering the TiO$_2$ photoelectrodes comprising light-scattering overlayer and dye-supporting underlayer, sufficient dye adsorption should be maintained to stabilize the performance of the resulting DSSCs. In the traditional dip-coating process, the dyes are attached to TiO$_2$ via dye concentration gradient-induced diffusion process, which results in relatively long dye-coating time of more than $\sim$ 24 h and unpredictable consumption of dye molecules [20,21]. The effective dye-adsorption process that uses dye solutions with relatively high concentrations and temperatures has been developed previously [22,23]. However, this process encounters some difficulties in controlling the dye adsorption and scale-up processes.

Therefore, in this study, we fabricate bilayered photoelectrode comprising dye-supporting underlayer and light-scattering overlayer and examine their effect on the efficiency of the resulting DSSCs. Specifically, the light-scattering overlayer and dye-supporting underlayer comprise 250 nm TiO$_2$ NPs (hereafter denoted as T250) and 25 nm TiO$_2$ NPs (hereafter denoted as T25), respectively. The thickness ratios of both light-scattering and dye-supporting layers are varied at T25:T250 = 10:0, 7:3, and 5:5 to obtain optimized photovoltaic performance. To deposit dyes on the bilayered TiO$_2$ photoelectrodes fabricated herein, a single-stage aerosol impactor is used, which facilitates the rapid deposition of controlled amount of dyes on the TiO$_2$ NPs through strong inertial impaction. The photovoltaic characteristics of DSSCs coated with N719 dyes using the impactor system are finally analyzed.

2. Experimental methods

2.1. Preparation of TiO$_2$ paste and thin films, photoelectrodes, and counter electrodes

First, the FTO glass (SnO$_2$/F, Pilkington, USA) was washed with acetone, distilled water, and ethanol; then, it was immersed in a mixed distilled water (20 mL) and TiOCl$_2$ (0.247 mL) solution heated at 70 °C to attach the TiO$_2$ NPs-accumulated layers on the glass surface. The viscous TiO$_2$ paste used for forming a TiO$_2$ thin film as a photoelectrode was prepared as follows. Ethyl cellulose (0.15 g) was dissolved in ethanol solution (5 mL) in a vial, and TiO$_2$ NPs (0.3 g), acetic acid (0.05 mL), and terpineol (1 g) were mixed in an ethanol solution (3 mL) in another vial. Then, the prepared solutions were separately ultrasonicated for 1 h, followed by mixing in a planetary mixer operated under the rotating speed of 2000 rpm for 4 min. TiO$_2$ paste was finally prepared after thermal evaporation of the residual ethanol. Subsequently, screen-printed TiO$_2$ thin films were fabricated on the pretreated FTO glass. Then, the TiO$_2$-based photoelectrode (0.4 cm width × 0.4 cm length) was heated at 500 °C in a convection oven for 30 min to sinter the TiO$_2$ NPs in the photoelectrode. For fabricating the counter electrodes, other FTO glasses were fabricated with two holes to inject the liquid electrolyte later; then, they were treated according to the abovementioned cleaning processes prior to conducting Pt-coating process using an ion sputter (E1010, Hitachi, Japan).

2.2. Aerosol impactor-assisted dye adsorption and assembly of DSSCs

The N719 dye solution ((Bu$_4$N)$_2$[Ru(Hdcbpy)$_2$-(NCS)$_2$], Solaronix, Switzerland) was prepared by first dispersing the dye powder in ethanol, followed by the preparation of dye aerosol droplets using an ultrasonic atomizer, as shown in Fig. 1. Generally, an aerosol impactor is expected to remove aerosol particles above a critical cutoff size and impact the collection plate owing to the large momentum [24]. When dye aerosols entered the impactor inlet with a certain flow rate, sheath air controlled by a mass flow controller was supplied to accelerate the dye aerosols toward the bottom of the impactor. When the total flow rate of sheath air and dye droplets was maintained at $\sim$ 30 L min^{-1}, nozzle width was 1 cm, distance between the nozzle and impaction plate was 1 cm, and nozzle length was 5 cm, the resulting cutoff size (D$_p$) of the dye aerosol droplets was calculated to be $\sim$ 9 µm [25] (see the specifications and pictures of single-stage impactor in **Figure S1** in the Supporting Information). Once the generated dye aerosols were accelerated toward the impaction plate, they were deflected by a 90° sharp turn in the air streamline and were seriously deviated from their trajectories, so that the dye aerosols above the critical cutoff size were collided and smeared through the TiO$_2$ NPs-based thin films coated on a FTO glass, which was installed on the bottom of impactor (see Fig. 1) [25–27]. The introduced aerosol droplets were continuously impacted to the TiO$_2$, and thus, chemical reactions took place between the dyes with carboxylate (–COOH) groups and TiO$_2$ NPs with hydroxyl (–OH) groups [28]. In contrast, the smaller dye droplets than the cutoff size were simply collected on a filter by following the air streamlines.

Both TiO$_2$-based photoelectrode and Pt-based counter electrode were stacked, and then a polymer film was inserted between them. The polymer film (Surlyn, DuPont, USA) was cut into a square shape with a square hole of 0.5 cm × 0.5 cm and 60 µm thickness was inserted in the geometric center, wherein the dye-coated TiO$_2$ layer was fitted. The photoelectrode/polymer film/counter electrode with a sandwich structure was clamped and heated at 120 °C for tight sealing. Subsequently, the AN-50 electrolyte (Solaronix, Zollikon, Switzerland) was supplied in the counter electrode.

2.3. Measurement and analysis of characteristics of DSSCs performance

The DSSCs performance was analyzed using a solar simulator (1.5 air mass, 1 sun; PEC-L11, Peccell Technologies, Inc., Japan). A standard Si photodiode-assisted detector was used to check the light intensity of solar simulator. Another solar simulator (1.5 air mass, 1 sun; Sun 2000, Abet Technologies Inc., USA) was used to characterize the incident photon-to-electron conversion efficiency (IPCE). To determine the dye-adsorption amount, the dye-coated TiO$_2$ thin films were dipped into a NaOH solution (0.1 mol L^{-1}) for dissolving the dyes. The resulting dye-dissolved solution was analyzed using the light absorbance of N719 dye dispersed using UV–Vis spectrometer (Cary 5000, Agilent, USA).

3. Results and discussion

The photoelectrode of DSSCs was assembled with the spherical TiO$_2$ NPs with the average particle size of $\sim$ 25 nm in diameter (see the SEM image of TiO$_2$ NPs in **Figure S2b** in the Supporting Information), which were accumulated on the surface of FTO glass as a thin film with $\sim$ 15 µm thickness (see the schematic and SEM images of TiO$_2$ NPs-accumulated thin film in Fig. 3**a and b**). Various gas flow conditions were analyzed in the impactor to obtain the enhanced DSSC efficiency as shown in Table 1. Herein, sheath refers to the carrier gas that controls the impaction velocity of the dye droplets to the TiO$_2$ layer located on the bottom of impactor (see Fig. 1). The total amount of gas flow rates was fixed to $\sim$ 30 L min^{-1}. The dye-adsorption amount (M$_{DA}$), short circuit current density (J$_{sc}$), and PCE increased when the dye droplet flow was
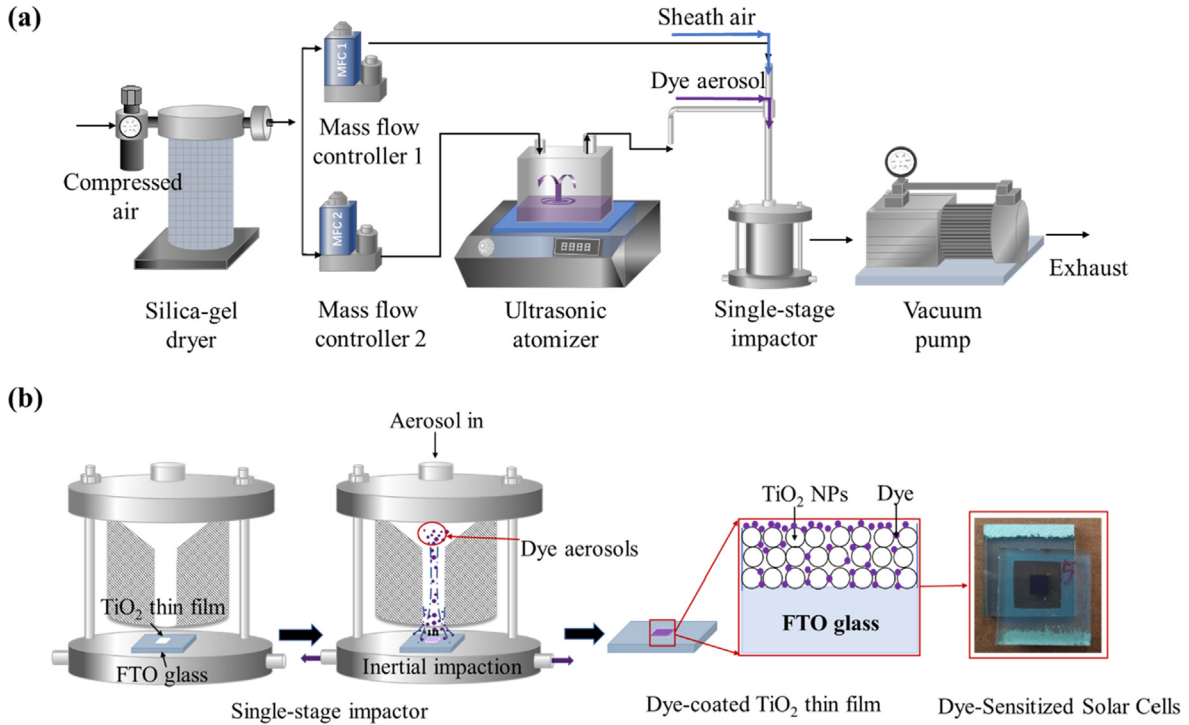
Fig. 1. (a) Schematic of the set up and operating system of dye aerosol impactor; and (b) schematic of the aerosol-coating processes of dye droplets impacted inertially on the TiO2 NPs-accumulated layer in the dye aerosol impactor system.

Table 1
Photovoltaic characteristics of various DSSCs assembled using the dye aerosol impactor operated under various gas flow conditions with a fixed coating duration of 180 min.

Ratio of flow rate (Sheath:Aerosol)	M_{DA} (10^{-6} mol cm^{-2})	J_{sc} (mA cm^{-2})	V_{oc} (V)	FF	PCE (%)
20:10	19.55 ± 0.99	11.46 ± 0.31	0.74 ± 0.03	0.72 ± 0.01	6.17 ± 0.41
15:15	20.52 ± 1.38	12.76 ± 0.29	0.72 ± 0.01	0.71 ± 0.02	6.47 ± 0.24
10:20	24.95 ± 0.84	14.68 ± 0.27	0.70 ± 0.01	0.69 ± 0.01	7.03 ± 0.45
5:25	23.99 ± 0.48	15.24 ± 0.46	0.70 ± 0.02	0.66 ± 0.03	7.00 ± 0.56

increased up to 20 L min^{-1}. Generally, J_{sc} is expressed as follows: $J_{sc} = q \times \eta_{light} \times \eta_{inj} \times \eta_{coll} \times I_o$, where q is the elementary charge, η_{light} is the light harvesting efficiency, η_{inj} is the electron injection efficiency from the dyes into TiO$_2$ conduction band, η_{coll} is the electron collection efficiency, and I_0 is the light intensity [29–31]. The increase in dye aerosol flow rate resulted in an increase in the aerosols impacting on the TiO$_2$-based photoelectrode, thereby increasing the values of J_{sc} and PCE. However, J_{sc} and PCE seemed to be saturated at aerosol flow rates higher than 20 L min^{-1}; this is because an excessive amount of dye aerosols was continuously deposited on the TiO$_2$-based photoelectrode, which was completely wet due to the failure of rapid solvent evaporation. Therefore, the wet surface made an unexpected shield for the direct impaction of continuously incoming dye aerosols.

The effect of coating duration on the resulting PCE of DSSCs composed of spherical TiO$_2$ NPs with a primary size of ~ 25 nm was also examined under various sheath and aerosol flow rates. The PCEs increased with an increase in the aerosol coating duration, followed by saturation at coating duration of > ~150 min, as shown in Fig. 2. With an increase in the coating duration, the dyes covered TiO$_2$ NPs with multilayers, which could hinder the electron transfer from dyes to TiO$_2$ NPs and can lower the PCE. The best PCE was observed under the mixing ratio of sheath:aerosol = 10:20 at the coating duration of 180 min.

To observe the effect of TiO$_2$ stacking structures on the efficiency of DSSCs, we fabricated a TiO$_2$ overlayer, with larger pri-
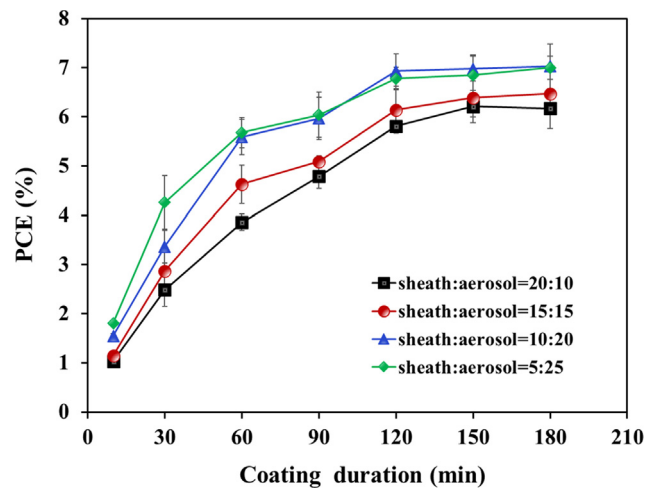
Fig. 2. Enhancement in the efficiency of DSSCs with varying coating duration and gas flow condition in the impactor.

mary particle size of ~ 250 nm (T250) as a light-scattering medium, on the top of a TiO$_2$ underlayer, with primary particle size of ~ 25 nm (T25) as a dye-supporting medium, in the photoelectrode (see the SEM images of top- and cross-sectional view of
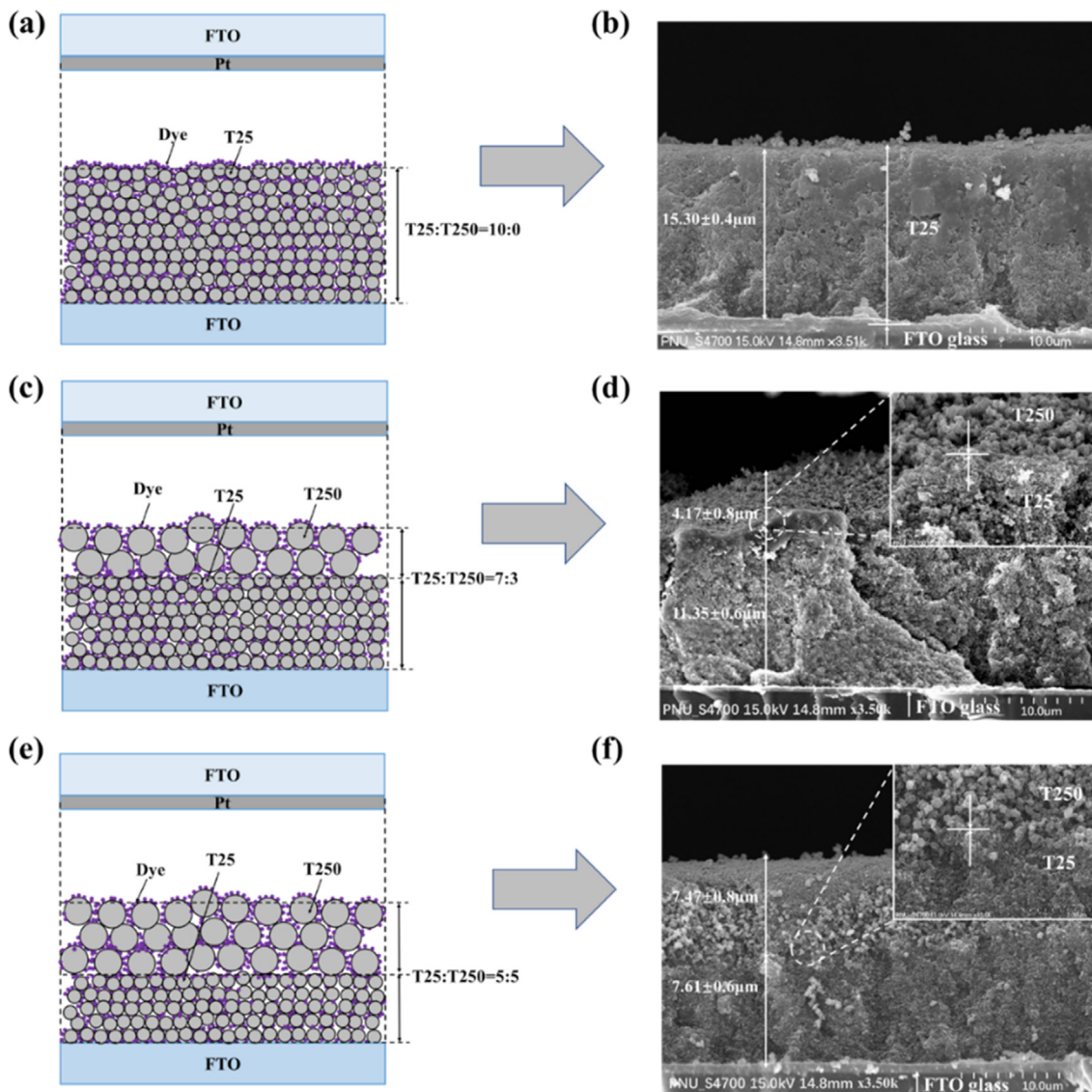
Fig. 3. Schematics and cross-sectional SEM images of three different types of TiO$_2$ thin films as photoelectrodes assembled in DSSCs: (a, b) Structure I (T25:T250 = 10:0); (c, d) structure II (T25:T250 = 7:3); and (e, f) structure III (T25:T250 = 5:5).

TiO$_2$ photoelectrode in **Figure S2** in the Supporting Information). Three different types of TiO$_2$ stacking structures were assembled on the FTO glass. The schematics and cross-sectional SEM images of photoelectrodes are shown in Fig. 3. The total thickness of TiO$_2$ thin films was generally close to approximately 15 μm. The TiO$_2$ stacking structures comprised three different thickness ratios (T25:T250) of 10:0, 7:3, and 5:5, for comparison. Structure I (i.e., T25:T250 = 10:0) was densely packed single layer of T25 (Fig. 3a **and b**). However, structures II (i.e., T25:T250 = 7:3) and III (i.e., T25:T250 = 5:5) clearly comprised double layer of T25 and T250 with different thicknesses (Fig. 3c-f), in which the T250 overlayer had larger pores than the T25 underlayer due to the presence of larger primary particles.

In order to examine the light-scattering effect of T250, UV − Vis diffuse reflectance spectra of three different types of TiO$_2$ thin films were measured as shown in Fig. 4a. It was observed that the structure II (i.e., T25:T250 = 7:3) and III (i.e., T25:T250 = 5:5)-based TiO$_2$ thin films exhibited the higher diffuse reflectance than structure I (i.e., T25:T250 = 10:0)-based TiO$_2$ thin film. This suggests that the presence of T250 in structures II and III played an important role as a light-scattering medium in the photoelectrodes (see the UV–Vis

diffused reflectance spectra of T25 and T250 for comparison in **Figure S3** in the Supporting Information). Furthermore, the structure II-based TiO$_2$ thin film exhibited the higher diffuse reflectance than structure III-based TiO$_2$ thin film. This is presumably because the excessive T250 in structure III caused too much backscattering, which resulted in increasing the reflectivity of TiO$_2$ thin film. Fig. 4b shows UV–Vis absorption spectra for three different types of TiO$_2$ thin films. The structure II-based TiO$_2$ thin films exhibited higher light absorption than that of the structure I and III, indicating that the presence of optimized amount of T250 overlayer on top of T25 underlayer can act as an effective light scattering medium to occur multiple light scattering pathways so that the propagation distance of light can be extended in the photoelectrode.

Table 2 shows the photovoltaic characteristics of DSSCs incorporated with various TiO$_2$ stacking structures coated with N719 dyes using conventional dip-coating process and dye aerosol-coating process. The dye-adsorption amount for structure II- and III-based DSSCs was generally lesser than those for structure I-based DSSCs due to the presence of T250 with larger primary NPs in the overlayer. Although the amount of dye adsorption decreased using T250 overlayer in structure II-based DSSCs, the
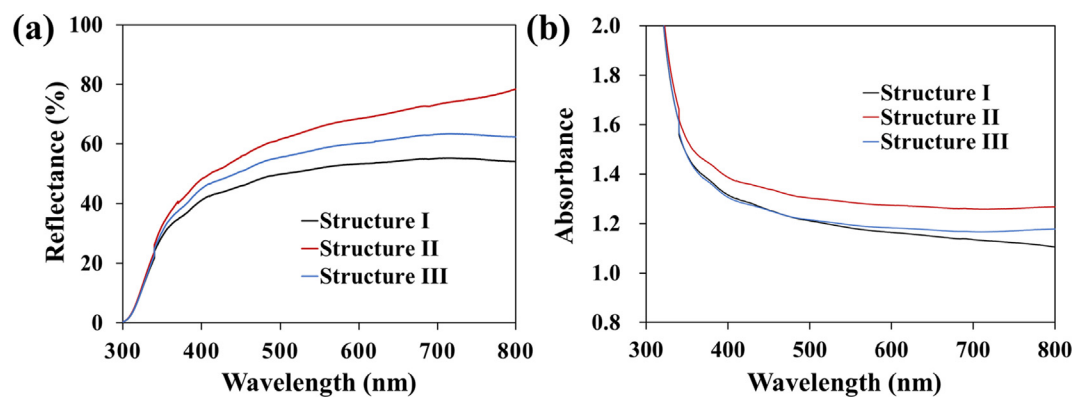
Fig. 4. (a) UV − Vis diffused reflectance spectra and (b) absorbance spectra of three different types of TiO$_2$ thin films: Structure I (T25:T250 = 10:0), structure II (T25: T250 = 7:3), and structure III (T25:T250 = 5:5).

Table 2
Photovoltaic characteristics of DSSCs composed of various TiO$_2$ stacking structures coated by N719 dyes using dip and aerosol-coating processes.

Dye-adsorption method	Optimized coating duration (min)	Structure of TiO$_2$ thin film	M$_{DA}$ (10^{-6} mol cm^{-2})	J$_{sc}$ (mA cm^{-2})	V$_{oc}$ (V)	FF	PCE (%)
Dip coating	1800	Structure I	21.90 ± 0.54	11.78 ± 0.47	0.69 ± 0.01	0.72 ± 0.11	5.67 ± 0.23
		Structure II	19.11 ± 0.27	13.31 ± 0.33	0.73 ± 0.02	0.69 ± 0.07	6.70 ± 0.12
		Structure III	16.29 ± 0.41	11.11 ± 0.24	0.69 ± 0.01	0.72 ± 0.05	5.53 ± 0.26
Aerosol coating	180	Structure I	24.95 ± 0.74	14.68 ± 0.27	0.70 ± 0.01	0.69 ± 0.01	7.03 ± 0.45
		Structure II	21.75 ± 0.35	15.04 ± 0.13	0.72 ± 0.03	0.68 ± 0.03	7.46 ± 0.17
		Structure III	19.35 ± 0.24	13.03 ± 0.45	0.73 ± 0.01	0.71 ± 0.09	6.83 ± 0.21

resulting PCE was enhanced. This suggests that the addition of optimized T250-based light-scattering overlayer on the top of T25-based dye-supporting underlayer in the photoelectrode could promote the light harvesting of DSSCs. However, the addition of excessive T250 overlayer on the top of T25 underlayer in structure III (T25:T250 = 5:5) could deteriorate the efficiency of DSSCs because the specific surface area of TiO$_2$ stacking structure was decreased by reducing the T25 layer, which significantly decreased the dye-adsorption amount. The optimized TiO$_2$ double layer-based thin film for the case of conventional dip-coating process had thickness ratio of 7:3 (i.e., structure II, PCE = 6.70 ± 0.12%), thereby increasing the PCE of DSSCs by 18% than those of structure I-based DSSCs (i.e., PCE = 5.67 ± 0.23%). Furthermore, the best PCE (7.46 ± 0.17%) for structure II-based DSSC assembled under the aerosol-coating process for ∼ 180 min was ∼ 32% higher than that of structure I-based DSSC (PCE = 5.67 ± 0.23%) and 10 times faster than the dip-coating process (∼1800 min). This suggests that the aerosol-coating process can rapidly and effectively coat the TiO$_2$ NPs with dyes via aerosol impaction in depth. In addition, the presence of T250 overlayer on the top of T25 underlayer with an optimized thickness ratio can considerably promote the light harvesting in DSSCs. The electrochemical impedance spectroscopy (EIS) and electron mobility analyses using Nyquist and Bode plots were additionally provided to analyze the photovoltaic performance of various DSSCs assembled using dip- and aerosol-coating processes in **Figure S4** and **Table S1** in the Supporting Information.

After determining the optimized TiO$_2$ stacking structure of T25: T250 = 7:3, we qualitatively observed the dye adsorption by varying the coating duration. Fig. 5 shows the images of TiO$_2$ layers coated with N719 dyes using dip- and aerosol-coating processes operated under various coating durations. The color was lighter for shorter coating durations because the small amount of dyes

was adsorbed. When the coating duration increased, the color darkened rapidly from light pink to dark purple due to the increasing amount of dye getting adsorbed. This suggests that TiO$_2$ could be sufficiently coated with dyes in such a relatively short coating duration (< ∼180 min) because the dye aerosols accelerated in the impactor had strong inertial impaction and they rapidly penetrated through the porous TiO$_2$ layer. However, for the case of conventional dip-coating process, the color of TiO$_2$ layer changed very slowly from light pink to dark purple for coating duration of < ∼1800 min. During the dip-coating process, the diffusion process of dye molecules occurred very slowly. In the long-term immersion of dye solution, the adsorption and desorption of dyes on the porous TiO$_2$ layer occurs at the same time, i.e., the local high concentration of dyes on the TiO$_2$ may diffuse into the dye solution, resulting in lowering the dye-adsorption rate of TiO$_2$ layer.

To examine the uniformity of dye deposition on TiO$_2$ NPs-accumulated thin films (T25:T250 = 7:3), we performed SEM analysis as shown in Fig. 6. The primary TiO$_2$ NPs were compactly accumulated on the surface of FTO glass without a dye coating process (Fig. 6**a-c**). When the TiO$_2$ thin film was treated with the conventional dip-coating process for the coating duration of ∼ 1800 min, the upper layer was uniformly coated with dyes, but the amount of dyes adsorbed in depth seemed to be decreased to some extent (Fig. 6**d-f**). However, when the TiO$_2$ thin film was treated with the aerosol-coating process, the dye molecules were completely deposited throughout the TiO$_2$ thin film and reached to the FTO glass due to strong inertial impaction (Fig. 6**g-i**). This suggests that the TiO$_2$ NPs-accumulated thin films can be uniformly coated in-depth with the introduced dye molecules using the aerosol-coating process.

The effect of varying the coating duration on the performance of DSSCs incorporated with the TiO$_2$ stacking structure II (i.e., T25: T250 = 7:3) was examined (Fig. 7). The PCE increased with increas-
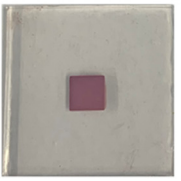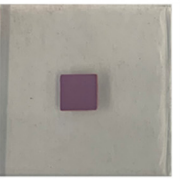
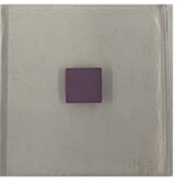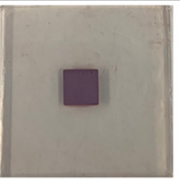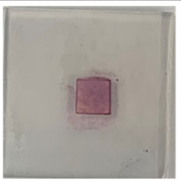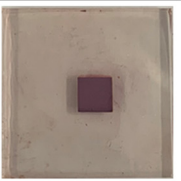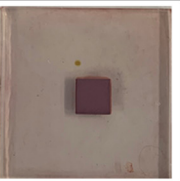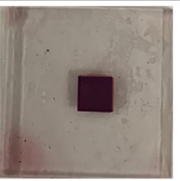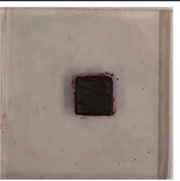| Coating duration (min)	10	60	180	600	1800
Dip Coating					

Coating duration (min)	10	60	120	150	180
Aerosol coating					

Fig. 5. TiO$_2$ thin films (T25:T250 = 7:3) coated with N719 dyes using dip- and aerosol-coating processes under various coating durations.
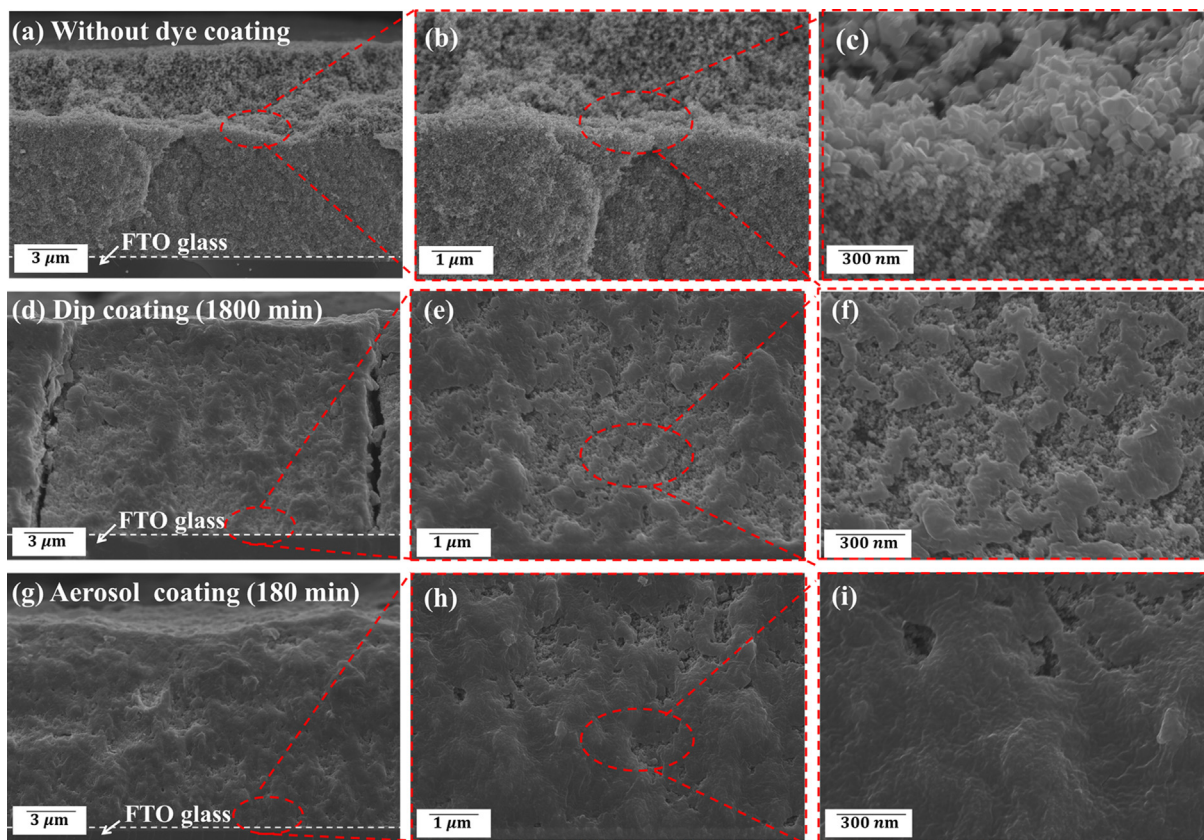

Fig. 6. Cross-sectional SEM images of TiO$_2$ thin film (a, b, c) without dye coatingprocess, (d, e, f) with dip- coating process for 1800 min, and (g, h, i) with aerosol-coating process for 180 min.
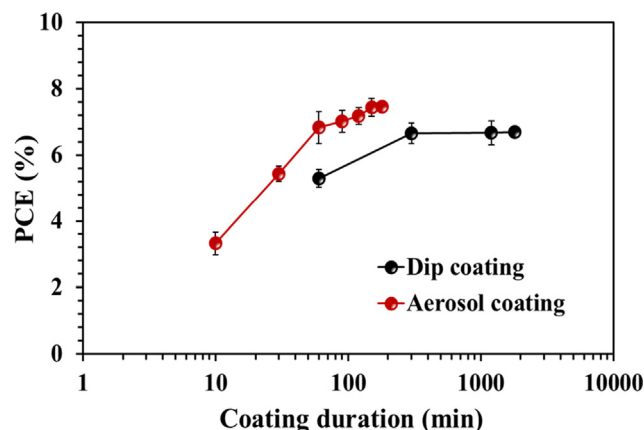
Fig. 7. Enhancement in the PCE of DSSCs incorporated with a T25/T250 double layered stacking structure (i.e., T25:T250 = 7:3) and coated with N719 dyes using dip-coating process and aerosol-coating process by varying coating duration, respectively.
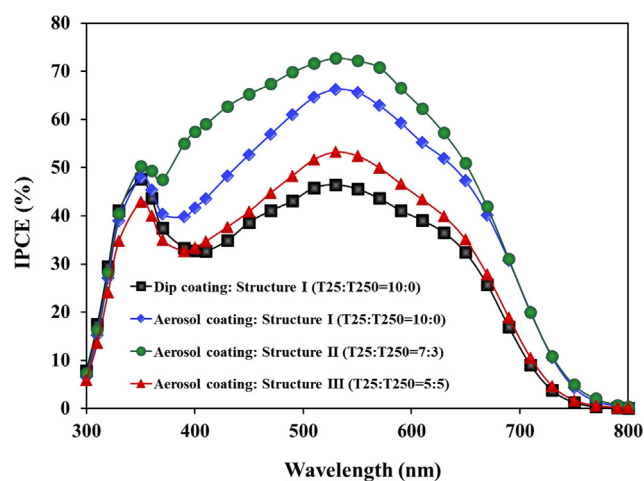

Fig. 8. IPCE spectra of DSSCs incorporated with various TiO_2 stacking structures coated with N719 dyes using aerosol- and dip-coating process with the coating duration of ~ 180 and ~ 1800 min, respectively.

ing the coating duration. The PCEs of DSSCs assembled by aerosol-coating process were much higher than those of DSSCs assembled by conventional dip-coating process for the same coating durations. This confirms that effective TiO_2 stacking structures assembled using the aerosol-coating process could significantly improve the DSSCs efficiency by rapid dye adsorption and effective light trapping effects.

The IPCE spectra of DSSCs assembled with various TiO_2 stacking structures, which were coated with N719 dyes using the aerosol-coating process for the optimized coating duration of ~ 180 min, are shown in Fig. 8. IPCE spectra of dip-coating process for the optimized coating duration of ~ 1800 min and structure I (i.e., T25:T250 = 10:0)-based DSSCs was also provided for comparison. The aerosol-coating process-assisted DSSCs clearly exhibited better IPCE than those exhibited by process-assisted DSSCs. In addition, the IPCE spectra of DSSCs incorporated with structure II (i.e., T25:T250 = 7:3)-based photoelectrode was the best among all the other TiO_2 stacking structures. These results confirmed that the rapid dye adsorption on the TiO_2 incorporated with optimized stacking structures comprising dye supporting and light-scattering layers could significantly improve the photovoltaic characteristics of DSSCs.

4. Conclusions

In this study, we investigated the combined effects of dye aerosol impaction and TiO_2 stacking structures on the resulting photovoltaic characteristics of DSSCs. By optimizing the gas flow conditions in the impactor, we achieved faster and more effective dye adsorption in the TiO_2-based photoelectrodes of DSSCs than those achieved via conventional dip-coating process. In addition, various T25/T250-based double layers comprising TiO_2 layer with large primary particles (T250) accumulated on the top of TiO_2 layer with small primary particles (T25) were tested to increase the light trapping effect in the photoelectrodes. For conventional dip-coating process, the optimized TiO_2 double layer-based thin film had a mixing ratio of T25:T250 = 7:3, which increased the PCE of DSSC by 18% (i.e., PCE = 5.67% and 6.70% for T25 single layer-based DSSC and T25/T250 double layer (T25:T250 = 7:3)-based DSSC, respectively). However, when T25/T250 double layer-based thin film was coated with N719 dyes using the aerosol impactor, the resulting PCE of DSSC increased by 32% (PCE = 7.46% for T25/T250 double layer (T25:T250 = 7:3)-based DSSC for the case of aerosol impactor). This suggests that the efficiency of DSSCs can be significantly enhanced by employing effective TiO_2 stacking structures comprising light-scattering and dye-supporting layers in the photoelectrodes, which are coated by strong dye aerosol impaction.

Funding Sources

Declaration of Competing Interest

The authors declare that they have no known competing financial interests or personal relationships that could have appeared to influence the work reported in this paper.

Appendix A. Supplementary material

Supplementary data to this article can be found online at https://doi.org/10.1016/j.apt.2021.11.019.

References

[1] B. O'Regan, M. Grätzel, A low-cost, high-efficiency solar cell based on dye-sensitized colloidal TiO_2 films, Nature 353 (6346) (1991) 737–740.
[2] A. Hagfeldt, M. Grätzel, Molecular photovoltaics, Acc. Chem. Res. 33 (5) (2000) 269–277.
[3] A. Hagfeldt, G. Boschloo, L. Sun, L. Kloo, H. Pettersson, Dye-sensitized solar cells, Chem. Rev. 110 (11) (2010) 6595–6663.
[4] J. Gong, K. Sumathy, Q. Qiao, Z. Zhou, Review on dye-sensitized solar cells (DSSCs): Advanced techniques and research trends, Renew. Sustain. Energy Rev. 68 (2017) 234–246.
[5] M. Grätzel, Dye-sensitized solar cells, J. Photochemistry and Photobiology C 4 (2) (2003) 145–153.
[6] S. Ito, T.N. Murakami, P. Comte, P. Liska, C. Grätzel, M.K. Nazeeruddin, M. Grätzel, Fabrication of thin film dye sensitized solar cells with solar to electric power conversion efficiency over 10%, Thin Solid Films 516 (14) (2008) 4613–4619.
[7] M. Grätzel, J.R. Durrant, Dye-sensitized mesoscopic solar cells, in: M.D. Archer, A.J. Nozik (Eds.), Nanostructured and photoelectrochemical systems for solar photon conversion, Imperial College Press, London, 2008, pp. 503–536.
[8] H. Chen, N.a. Li, Y.-H. Wu, J.-B. Shi, B.-X. Lei, Z.-F. Sun, A novel cheap, one-step and facile synthesis of hierarchical TiO_2 nanotubes as fast electron transport

channels for highly efficient dye-sensitized solar cells, Adv. Powder Technol. 31 (4) (2020) 1556–1563.

[9] X. Luo, J.H. Kim, J.Y. Ahn, D. Lee, J.M. Kim, D.G. Lee, S.H. Kim, Electrospraying-assisted rapid dye molecule uptake on the surfaces of TiO$_2$ nanoparticles for speeding up dye-sensitized solar cell fabrication, Sol. Energy Mater. Sol. Cells 144 (2016) 411–417.

[10] M. Grätzel, Mesoporous oxide junctions and nanostructured solar cells, Curr. Opin. Colloid Interface Sci. 4 (4) (1999) 314–321.

[11] M.K. Nazeeruddin, E. Baranoff, M. Grätzel, Dye-sensitized solar cells: A brief overview, Sol. Energy 85 (6) (2011) 1172–1178.

[12] K. Sharma, V. Sharma, S.S. Sharma, Dye-sensitized solar cells: Fundamentals and current status, Nanoscale Res. Lett. 13 (2018) 381.

[13] X.-D. Qiao, X.-Y. Ye, Y.-H. Wu, L.-J. Ma, B.-X. Lei, Z.-F. Sun, Tunable synthesis of mesoporous titania with different morphologies for dye-sensitized solar cells, Adv. Powder Technol. 32 (1) (2021) 99–105.

[14] M. Ye, X. Wen, M. Wang, J. Iocozzia, N. Zhang, C. Lin, Z. Lin, Recent advances in dye-sensitized solar cells: from photoanodes, sensitizers and electrolytes to counter electrodes, Mater. Today 18 (3) (2015) 155–162.

[15] H.S. ElBatal, S. Aghazada, S.A. Al-Muhtaseb, M. Grätzel, M.K. Nazeeruddin, Quasi-solid-state dye-sensitized solar cells based on Ru(II) polypyridine sensitizers, Energy Technology 4 (3) (2016) 380–384.

[16] S. Hore, C. Vetter, R. Kern, H. Smit, A. Hinsch, Influence of scattering layers on efficiency of dye-sensitized solar cells, Sol. Energy Mater. Sol. Cells 90 (9) (2006) 1176–1188.

[17] H. Xu, X. Tao, D.-T. Wang, Y.-Z. Zheng, J.-F. Chen, Enhanced efficiency in dye-sensitized solar cells based on TiO$_2$ nanocrystal/nanotube double-layered films, Electrochim. Acta 55 (7) (2010) 2280–2285.

[18] T.G. Deepak, G.S. Anjusree, S. Thomas, T.A. Arun, S.V. Nair, A. Sreekumaran Nair, A review on materials for light scattering in dye-sensitized solar cells, RSC Adv. 4 (34) (2014) 17615–17638.

[19] M.N. Mustafa, S. Shafie, M.H. Wahid, Y. Sulaiman, Light scattering effect of polyvinyl-alcohol/titanium dioxide nanofibers in the dye-sensitized solar cell, Sci. Rep. 9 (2019) 14952.

[20] S.N.A. Zaine, N.M. Mohamed, M. Khatani, A.E. Samsudin, M.U. Shahid, Improving the light scattering efficiency of photoelectrode dye-sensitized solar cell through optimization of core-shell structure, Mater. Today 19 (2019) 220–229.

[21] K.-J. Hwang, W.-G. Shim, Y. Kim, G. Kim, C. Choi, S.O. Kang, D.W. Cho, Dye adsorption mechanisms in TiO$_2$ films, and their effects on photodynamic and photovoltaic properties in dye-sensitized solar cell, PCCP 17 (2015) 21974.

[22] F. Hirose, M. Shikaku, Y. Kimura, M. Niwano, IR study on N719 dye adsorption with high temperature dye solution for highly efficient dye-sensitized solar cells, Journal of Electrochemical Society 157 (11) (2010) B1578, https://doi.org/10.1149/1.3485036.

[23] A. Hinsch, J.M. Kroon, R. Kern, I. Uhlendorf, J. Holzbock, A. Meyer, J. Ferber, Long-term stability of dye-sensitized solar cells, Prog. Photovoltaics Res. Appl. 9 (6) (2011) 425–483.

[24] M. Son, S. Lim, G. Sung, T. Kim, Y. Ha, K. Choi, W.G. Shin, Development of a novel aerosol impactor utilizing inward flow from a ring-shaped nozzle, J. Aerosol Sci. 85 (2015) 1–9.

[25] V.A. Marple, K. Willeke, Impactor design, Atmos. Environ. 10 (10) (1976) 891–896.

[26] G.J. Newton, O.G. Raabe, B.V. Mokler, Cascade impactor design and performance, J. Aerosol Sci. 8 (5) (1977) 339–347.

[27] V.A. Marple, B.Y.H. Liu, On fluid flow and aerosol impaction in inertial impactors, J. Colloid Interface Sci. 53 (1) (1975) 31–34.

[28] K. Murakoshi, G. Kano, Y. Wada, S. Yanagida, H. Miyazaki, M. Matsumoto, S. Murasawa, Importance of binding states between photosensitizing molecules and the TiO$_2$ surface for efficiency in a dye-sensitized solar cell, J. Electroanal. Chem. 396 (1-2) (1995) 27–34.

[29] Y.P. Lin, S.Y. Lin, Y.C. Lee, Y.W. Chen-Yang, High surface area electrospun prickle-like hierarchical anatase TiO$_2$ nanofibers for dye-sensitized solar cell photoanodes, J. Mater. Chem. A 1 (34) (2013) 9875, https://doi.org/10.1039/c3ta10925a.

[30] Y. Wang, T. Matsushima, H. Murata, A. Fleurence, Y. Yamada-Takamura, R. Friedlein, Molecular order, charge injection efficiency and the role of intramolecular polar bonds at organic/organic heterointerfaces, Org. Electron. 13 (10) (2012) 1853–1858.

[31] M. Pastore, A. Selloni, S. Fantacci, F. De Angelis, Electronic and optical properties of dye-sensitized TiO$_2$ interfaces, in: C. Di Valentin, S. Botti, M. Cococcioni (Eds.), First Principles Approaches to Spectroscopic Properties of Complex Materials, Springer, Berlin, 2014, pp. 1–45.